Emissivity of solar cell cover glass calculated from infrared reflectance measurements

Indra Subedi[a], Timothy J Silverman[b], Michael G. Deceglie[b], and Nikolas J. Podraza[a]

[a]*Department of Physics & Astronomy and Wright Center for Photovoltaics Innovation & Commercialization, University of Toledo, Toledo, OH 43606 USA*

[b]*National Renewable Energy Laboratory, Golden, CO 80401 USA*

Abstract

The thermal emissivity of solar cell cover glasses with differences in glass composition or manufacture and surface texture are evaluated using specular and specular+diffuse infrared reflectance at the different angle of incidences. Non-textured and textured glasses all exhibit similar emissivity at all angles of incidence regardless of composition and patterning. Both diffuse and specular reflectance must be included for textured glass at any angle of incidence and may be needed for planar glass at a high angle of incidences to properly determine emissivity.

Keywords: - Thermal emissivity, soda lime glass, covering glass for PV, infrared reflectance, silicon PV module

1. Introduction

The emissivity of any material quantifies its ability to emit energy as thermal radiation. Glass is a very efficient absorber and emitter for thermal radiation and is used as the front cover for most photovoltaic (PV) modules. In a commercial silicon PV module, the cover glass thickness is ~ 3 mm. This front cover glass is the thickest medium that incident light travels through before reaching the solar cell where it is ultimately absorbed and generates current. Glass used in buildings, windows, and PV modules have different requirements. For buildings, glass with low transmittance may be used to reject heat and reduce glare. However, glass used in PV panels should be ultra-clear, with a high transmittance over the portion of the solar irradiance spectrum that the cell can convert to photocurrent. One way this is achieved is low iron content [1]. Spectral and thermal properties of glass in the wavelength range near the peak blackbody irradiance for an object near room temperature are particularly important for PV because glass emits thermal radiation in that range enabling the solar cell to remain cooler and operate at higher efficiency [2]. The relation between emissivity and infrared optical properties may also be used to make glasses a nearly perfect blackbody via coatings [3]. Cover glass emissivities are used for modeling the thermal response of PV devices, with the goal of reducing solar cell operating temperature [4]. Control of cover glass thermal emissivity has been suggested for radiative cooling in PV modules [5], by maximizing the emission from the glass to reduce module temperature enabling higher operating efficiency.

Spectral emissivity, $\varepsilon(\lambda,T)$, of materials is typically determined by two methods [6]. One is based on Planck's law, in which emissivity is calculated by comparing spectral radiation intensities measured from the sample and a blackbody by a radiation thermometer or

* Corresponding author.
E-mail address: nikolas.podraza@utoledo.edu (N. J. Podraza)

spectrometer. The second is an indirect approach to evaluate absorptance by measuring spectral reflectance and applying Kirchhoff's law. According to Kirchhoff's law [7], spectral emissivity of a material is equivalent to spectral absorptance at thermal equilibrium. This indirect method is the most widely used to evaluate the emissivity of both bare and coated glasses at ambient temperature [8]. Earlier thermal radiative properties of glass are evaluated up to the far infrared range [9-11] but most of these studies use only specular reflectance measurements to calculate the absorptance and related emissivity.

In this contribution, we have calculated emissivity from specular and specular+diffuse reflectance measurements of three commercial low iron soda lime glasses (SLG) commonly used in PV modules: Solite™, Diamant®, and Pilkington. We have also evaluated differences in emittance based on the assumptions used for its calculation including the assumed blackbody temperature. Diamant® and Pilkington are colorless float glasses while Solite™ is a textured glass formed with a regular diamond pattern on one side and having random texture on the other. The randomly textured surface of this glass, referred as "sun side", faces the sun and the diamond pattern side faces the silicon solar cell when used in the PV module. Only the sun side of Solite™ glass is relevant for the measurements here. During the manufacturing of float glasses, a certain amount of tin can diffuse into one side of the glass [12] in contact with and floating upon the liquid tin. Optical properties of the tin side are slightly different than the other side (air side) over the visible to ultraviolet range [12, 13]. The difference is substantial in the infrared region, but the tin-rich region is small in overall thickness (~30 nm) compared to the remainder of the bulk glass [13]. Diamant® and Pilkington both have tin-rich sides and another side in contact with air during the float fabrication process. For float glass, usually the tin-rich side faces the solar cell and the air side faces the sun. We evaluated emissivities of these three different types of glasses used for covering PV to identify variations in thermal emissivity with manufacture, surface compositions / structure, and infrared reflectance measurement configuration.

2. Infrared Measurement of Samples

Total integrated (specular+diffuse) unpolarized angular reflectance, $R(\lambda)$, and transmittance, $T(\lambda)$, from 1.69 to 25.4 μm of the sun-facing side of Solite™ glass and both sides of Diamant® float glass are measured at 8˚, 35˚, 55˚, 60º, 65º, 70º, 75º, and 80˚ angles of incidence with respect to the sample normal in a hemispherical directional reflectometer (SOC-100 HDR, Surface Optics Corporation) coupled with the Nicolet Fourier transform infrared (FT-IR) spectrophotometer. This SOC-100 HDR uses a gold-coated hemiellipsoid to illuminate the sample by a radiation source. The reflection from the sample enters a Nicolet FTIR by using an overhead mirror at a user-defined angle [14]. Reference spectra are obtained from a specular gold standard for reflectance and straight-through measurement without a sample for transmittance for this instrument. Uncertainty for specular+diffuse measurements are 0.01 and 0.05 for near normal and for 60º angles of incidences, respectively. A rotating compensator ellipsometer [15] (IR-VASE®, J.A. Woollam Co.) with a spectral range from 1.69 to 30 μm is used to acquire polarized specular reflectance for all glass samples at 35˚, 55˚, 60º, 65º, 70º, 75º, and 80˚ angles of incidence relative to the sample normal. The IR-VASE® contains a Michelson interferometer with an IR transmitting beamsplitter, a silicon carbide Globar source, a dual-

rhomb achromatic rotating compensator, a wire grid polarizer, and a deuterated triglycine sulfate detector [16]. Reflectance data are obtained with a 16 cm^{-1} resolution. A gold mirror is used to measure a baseline before each specular measurement. Instrumental errors for specular measurements are 0.016 and 0.014 for 80º and 35º angles of incidences, respectively. Unpolarized reflectance is obtained by measuring the reflectance of light polarized parallel (p, R_p) and perpendicular (s, R_s) with respect to the plane of incidence followed by averaging, i.e. $R = (R_s + R_p) / 2$. Vecco Dektak 150 Stylus Profiler is used for surface profiling of sun side surface of Solite™ glass.

3. Results and Discussion

Specular reflection is generated by a smooth surface and diffuse reflection by sufficiently rough or textured surfaces. Total reflectance is the sum of specular and diffuse reflectances. In our case, the hemispherical directional reflectometer measures total reflectance while the ellipsometer measures only specular reflectance. We measured the emissivity of both the sun side and cell side of float glasses to see any differences in emissivity stemming from variations in reflectance for the tin and air sides. Directional spectral emissivity, $\varepsilon(\lambda,\theta)$, is evaluated from the $R(\lambda)$ and $T(\lambda)$ using $\varepsilon(\lambda, \theta) = 1 - T(\lambda, \theta) - R(\lambda, \theta)$. At long wavelengths in the infrared region, near the peak of the 300 K blackbody emission spectrum of an object at ambient temperature, glass is opaque so $T(\lambda, \theta) = 0$. Specular and specular+diffuse reflectance measurements from both sides of Diamant® float glass are shown in Fig. 1(a) and 1(b) for common measured angles. The specular and specular+diffuse measurements are qualitatively similar for both sides of the sample except some variation in magnitude possibly due to instrumental error at higher angles of incidence measured. Additionally, it should be noted that even nominally planar glass may have non-idealities arising during production or handling introducing a non-specular reflectance component particularly at high angles of incidence. The angular reflectance from both sides of Pilkington glass is nearly superimposed as shown in Fig. 2 and has almost the same spectral reflectance as Diamant®.

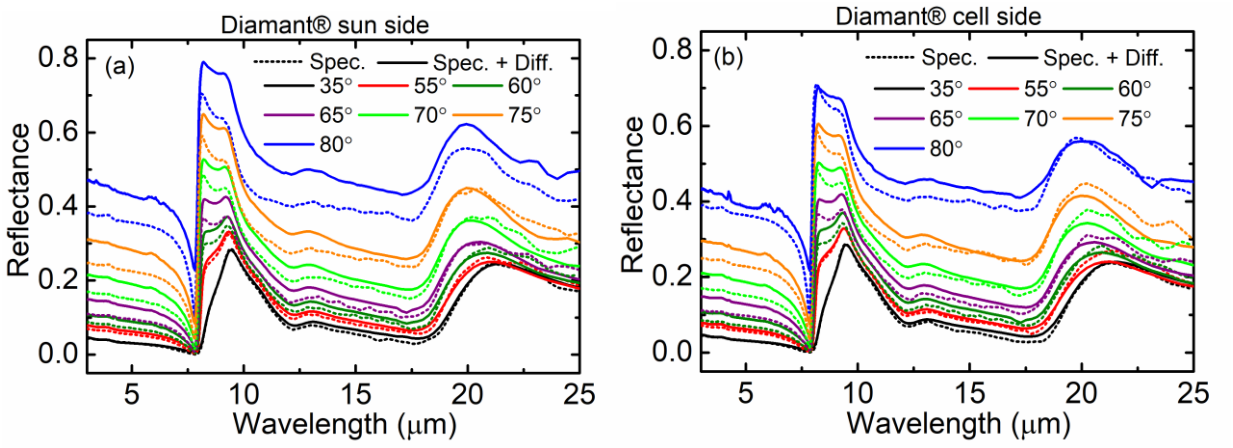

Fig. 1. Specular and specular+diffuse reflectance of the sun- (a) and cell-facing (b) sides of Diamant® glass as functions of angles of incidence.

In the case of non-textured glasses like Diamant® and Pilkington, only specular reflectance measurements should be necessary as diffuse reflectance is negligible. However, for Solite™ glass both the diffuse and specular components must be included due to scattering by the surface texture. The average height profile for the sun side of Solite™ glass is ~2.5 μm. Fig. 3 shows a substantial difference between specular and specular+diffuse reflectance for the sun-facing side of Solite™ glass at the common measured angles relative to that observed for Diamant®.

The total directional emissivity (emittance) is calculated from directional spectral emissivity weighted by the blackbody spectrum over a wavelength range, λ_1 to λ_2, at a given temperature [6, 17] by:

$$\varepsilon(\theta,T) = \frac{\int_{\lambda_1}^{\lambda_2} \varepsilon(\lambda,\theta)\, I_b(\lambda,T) d\lambda}{\int_{\lambda_1}^{\lambda_2} I_b(\lambda,T) d\lambda} \qquad (1),$$

where $I_b(\lambda, T)$ is the blackbody irradiance distribution and $\varepsilon(\lambda,\theta)$ is the directional spectral emissivity. Here we consider 283 and 300 K blackbody irradiances and 3 to 25 μm wavelength ranges for integration. Aside from ultraviolet absorption, PV glasses may be not substantially absorbing at wavelengths less than ~3 μm, so only wavelengths greater than 3 μm are included in the integration range. Calculated total directional emissivity at 300 K for the different glasses are shown in Table 1 and Fig. 4(a). Similar values at each angle of incidence are obtained for all non-textured glasses regardless of the sample side measured and its manufacturer. The small variation in emittance values for the non-textured glasses, between the cell-facing side and sun-facing side for Diamant® and Pilkington, may be due to instrumental variations as both values for each pair are within the 0.014 to 0.016 error range for these specular measurements.

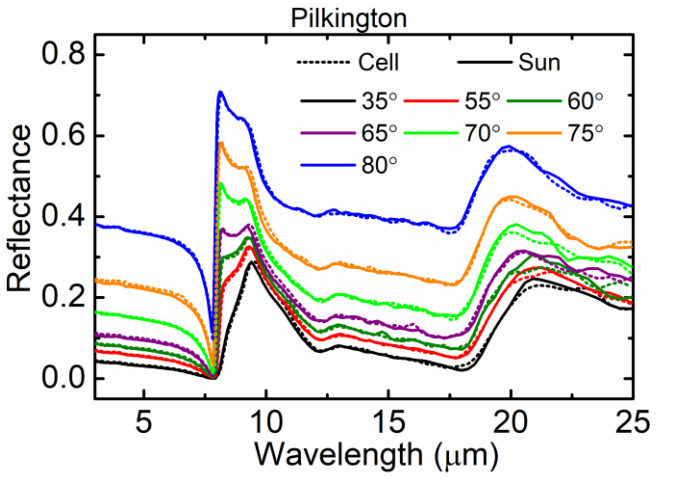

Fig. 2. Specular reflectance of the cell- and sun-facing sides of Pilkington glass as functions of angles of incidence.

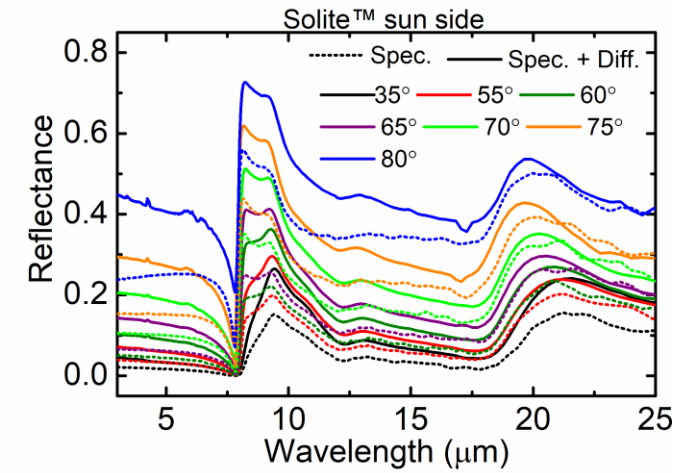

Fig. 3. Specular and specular+diffuse angular reflectance spectra of the sun-facing side of Solite™ glass.

For textured Solite™ glass, using only specular reflectance overestimates emissivity as the detector collects only a fraction of the total reflectance and results in erroneously high absorptance. When specular+diffuse reflectance is used instead, the appropriate absorptance is obtained, and comparable emissivity is observed at most angles of incidence relative to the non-textured glasses. This substantial difference illustrates the importance of properly including diffuse reflectance in the determination of emissivity, particularly at high angles of incidence.

Smaller values of emissivity from specular+diffuse measurements of Diamant® glass in comparison to the specular measurement alone at angles greater than 60° could arise from reduced sensitivity in the hemispherical directional reflectance system at high angles of incidence [18]. In some cases, the specular reflectance is higher than specular+diffuse at higher wavelengths as shown in Fig. 1(a), Fig. 1(b), and Fig. 3. Considering these comparisons, it is possible that the hemispherical directional reflectometer is not measuring full reflectance of all glasses at high angles of incidence. Also, measurements from the FTIR ellipsometer have larger experimental error at higher angles of incidence for longer wavelengths. These instrumental limitations may cause some differences between the expected specular and specular+diffuse measurement results. There may be other sources for these subtle variations such as slight offsets in the angles of incidence, different baselines, and different ambient measurement conditions between two instruments.

Emittance is also predicted for SLG using complex index of refraction spectra, $N(\lambda) = n(\lambda) + ik(\lambda)$. R_s and R_p are calculated using the Fresnel equations and spectra in $N(\lambda)$ for SLG [13]. The polarized reflectance at air / semi-infinite glass interface are:

$$R_s = \left| \frac{\cos\theta_i - \sqrt{N_g^2 - \sin^2\theta_i}}{\cos\theta_i + \sqrt{N_g^2 - \sin^2\theta_i}} \right|^2 \quad \text{and} \quad R_p = \left| \frac{N_g^2\cos\theta_i - \sqrt{N_g^2 - \sin^2\theta_i}}{N_g^2\cos\theta_i + \sqrt{N_g^2 - \sin^2\theta_i}} \right|^2 \qquad (2),$$

where N_g is the complex index of refraction for SLG and θ_i is the angle of incidence. Emittance as a function of angle of incidence calculated from reference N_g for SLG [13], Equation 2, Kirchhoff's law, and Equation 1 is also shown in Fig. 4(a). These calculated values are in close agreement with the measured emissivity for non-textured glasses at all angles.

Partial hemispherical emissivity ($\Delta\varepsilon_h$) is evaluated from directional total emissivity as described in Ref. [2]

$$\Delta\varepsilon_h = \frac{\int_o^\theta \varepsilon(\theta,T)\,2\pi\sin\theta d\theta}{\int_o^\theta 2\pi\sin\theta d\theta} \qquad (3)\ .$$

Partial hemispherical emissivity integrated up to 80˚ angle of incidence give hemispherical emissivity which is shown in Table 2 and Figure 4(b). All glasses have almost the same hemispherical emissivity except when only considering the specular measurement of Solite™, which is not a physically realistic case.

Table 1
Weighted total thermal emissivity (ε) between 3 to 25 μm for Solite™, Diamant®, and Pilkington glasses.

	Specular + Diffuse Reflectance			Specular Reflectance				
Angle of incidence (˚)	ε Solite™ sun side	ε Diamant® sun side	ε Diamant® cell side	ε Solite™ sun side	ε Diamant® sun side	ε Diamant® cell side	ε Pilkington sun side	ε Pilkington cell side
8	0.89	0.89	0.89	-	-	-	-	-
35	0.89	0.89	0.88	0.94	0.89	0.89	0.89	0.89
55	0.86	0.85	0.86	0.91	0.86	0.86	0.86	0.86
60	0.83	0.83	0.83	0.89	0.84	0.84	0.84	0.84
65	0.79	0.79	0.79	0.86	0.81	0.81	0.81	0.81
70	0.74	0.73	0.74	0.80	0.76	0.75	0.76	0.76
75	0.66	0.64	0.66	0.74	0.68	0.68	0.69	0.68
80	0.53	0.48	0.52	0.63	0.56	0.56	0.56	0.56

Table 2
Partial hemispherical emissivity ($\Delta\varepsilon_h$) evaluated from total directional emissivity (ε) for Solite™, Diamant®, and Pilkington glasses.

	Specular + Diffuse Reflectance			Specular Reflectance				
Angle of incidence (˚)	$\Delta\varepsilon_h$ Solite™ sun side	$\Delta\varepsilon_h$ Diamant® sun side	$\Delta\varepsilon_h$ Diamant® cell side	$\Delta\varepsilon_h$ Solite™ sun side	$\Delta\varepsilon_h$ Diamant® sun side	$\Delta\varepsilon_h$ Diamant® cell side	$\Delta\varepsilon_h$ Pilkington sun side	$\Delta\varepsilon_h$ Pilkington cell side
8	0.89	0.89	0.89	-	-	-	-	-
35	0.89	0.89	0.89	0.94	0.89	0.89	0.89	0.89
55	0.87	0.87	0.87	0.92	0.87	0.87	0.87	0.87
60	0.87	0.86	0.87	0.92	0.87	0.87	0.87	0.87
65	0.86	0.85	0.85	0.91	0.86	0.86	0.86	0.86
70	0.84	0.84	0.84	0.89	0.85	0.85	0.85	0.85
75	0.82	0.81	0.82	0.88	0.83	0.83	0.83	0.83
80	0.79	0.78	0.79	0.85	0.80	0.80	0.80	0.80

Gentle *et al*. [2] empirically calculated directional emittance and partial hemispherical emissivity for both silica and float glasses. The directional emissivity obtained for Diamant®,

Pilkington, specular + diffuse for Solite™ glasses, and that calculated for SLG based on input $N_g(\lambda)$ as a function of angle of incidence follow the same behavior as Gentle *et al*. but are slightly higher. The small difference in emissivity values reported in Ref. [2] may be due to differences in $N_g(\lambda)$ spectra applied, the assumed blackbody temperature, or the integration wavelength range used as input for the calculation. For Ref. [2], the assumed blackbody temperature is 283 K and the integration range is 2.5 to 35 μm. Directional emissivity of all glasses evaluated here agree well with the angular emissivity of uncoated glass reported elsewhere [19, 20]. The hemispherical emissivity calculated here is greater than reported by Gentle *et al*. [2] which includes all angular term up to 90º but lesser than reported by Rubin [10]. Additionally, about 17% of the total blackbody irradiance lies beyond the maximum 25 μm wavelength measured here [21]. Slight differences in emissivity will occur if wavelengths greater than 25 μm are also considered in the calculation. This type of variation in emissivity based on wavelength integration range may be greater than the expected instrumental variations of 0.014 to 0.016 and 0.01 to 0.05.

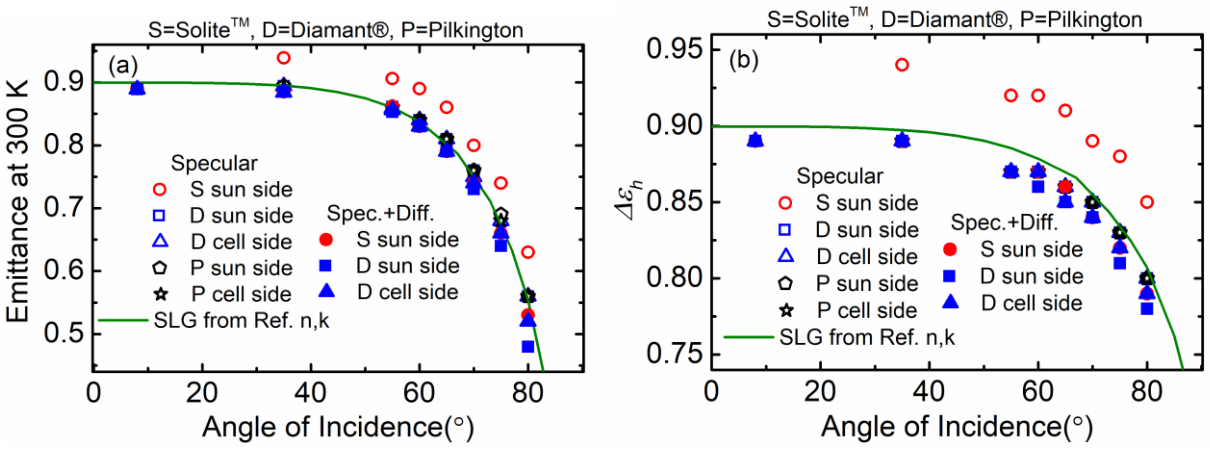

Fig. 4. (a) Thermal emittance of Solite™ (S), Diamant® (D), and Pilkington (P) glasses determined from the 3 to 25 μm wavelength range spectral emittance weighted by a 300 K room temperature blackbody. Specular S sun side points are derived from measurements ignoring diffuse reflectance. (b) Partial hemispherical emissivity ($\Delta\varepsilon_h$) for all glasses. Directional emittance and partial hemispherical emissivity are calculated from the complex index of refraction for reference soda lime glass [13].

There is also a small variation in emittance when weighted by 283 and 300 K blackbody irradiances. Emittance is slightly higher for a 300 K blackbody evaluated from 3 to 25 μm wavelength range compared to that weighted by a 283 K blackbody irradiance for the same integration range, with a maximum difference of 0.003. This value is within the expected instrumental variations, although larger differences in assumed blackbody temperature would result in greater differences.

4. Conclusions

Thermal emissivity has been calculated from specular and specular+diffuse infrared reflectance collected for textured and non-textured glasses used as cover glass in silicon PV modules. Ignoring diffuse reflectance for textured glass overestimates emissivity relative to its actual value. The impact of measurement configuration on emissivity is greater than that of glass manufacturer or sample side particularly at high angles of incidence. For higher angle reflectance measurement hemispherical reflectance should be used for planar glass as well to account for any unexpected source of non-specular scattering. Variation in irradiance from blackbodies near room temperature has a lesser impact on the weighted emissivity than the integration range applied.

Acknowledgements

This work was authored in part by Alliance for Sustainable Energy, LLC, the manager and operator of the National Renewable Energy Laboratory for the U.S. Department of Energy (DOE) under Contract No. DE-AC36-08GO28308. Funding provided by the U.S. Department of Energy's Office of Energy Efficiency and Renewable Energy (EERE) under Solar Energy Technologies Office (SETO) Agreement Number 30312. The views expressed in the article do not necessarily represent the views of the DOE or the U.S. Government. The U.S. Government retains and the publisher, by accepting the article for publication, acknowledges that the U.S. Government retains a nonexclusive, paid-up, irrevocable, worldwide license to publish or reproduce the published form of this work, or allow others to do so, for U.S. Government purposes.

References

[1] M.R. Vogt, H. Hahn, H. Holst, M. Winter, C. Schinke, M. Köntges, R. Brendel, P.P. Altermatt, Measurement of the Optical Constants of Soda-Lime Glasses in Dependence of Iron Content and Modeling of Iron-Related Power Losses in Crystalline Si Solar Cell Modules, IEEE Journal of Photovoltaics, 6 (2016) 111-118.

[2] A. Gentle, G. Smith, Is enhanced radiative cooling of solar cell modules worth pursuing?, Solar Energy Materials and Solar Cells, 150 (2016) 39-42.

[3] Y. Sun, Z. Zhou, X. Jin, X. Sun, M.A. Alam, P. Bermel, Radiative cooling for concentrating photovoltaic systems, in: Thermal Radiation Management for Energy Applications, International Society for Optics and Photonics, 2017, pp. 103690D.

[4] T.J. Silverman, M.G. Deceglie, I. Subedi, N.J. Podraza, I.M. Slauch, V.E. Ferry, I. Repins, Reducing Operating Temperature in Photovoltaic Modules, IEEE Journal of Photovoltaics, 8 (2018) 532-540.

[5] W. Li, Y. Shi, K. Chen, L. Zhu, S. Fan, A comprehensive photonic approach for solar cell cooling, ACS Photonics, 4 (2017) 774-782.

[6] H. Watanabe, J. Ishii, H. Wakabayashi, T. Kumano, L. Hanssen, Chapter 9 - Spectral Emissivity Measurements, in: T.A. Germer, J.C. Zwinkels, B.K. Tsai (Eds.) Experimental Methods in the Physical Sciences, Academic Press, 2014, pp. 333-366.

[7] J.R. Howel, R. Siegel, M. Mengűç, Thermal Radiation Heat Transfer 5th edition, 59-65, in, CRC Press, London, 2011.

[8] P. Honnerová, J. Martan, Z. Veselý, M. Honner, Method for emissivity measurement of semitransparent coatings at ambient temperature, Scientific Reports, 7 (2017).

[9] C.K. Hsieh, K. Su, Thermal radiative properties of glass from 0.32 to 206 μm, Solar Energy, 22 (1979) 37-43.

[10] M. Rubin, Optical properties of soda lime silica glasses, Solar Energy Materials, 12 (1985) 275-288.

[11] P. Van Nijnatten, M. Hutchins, N. Kilbey, A. Roos, K. Gelin, F. Geotti-Bianchini, P. Polato, C. Anderson, F. Olive, M. Köhl, Uncertainties in the determination of thermal emissivity by measurement of reflectance using Fourier transform spectrometers, Thin Solid Films, 502 (2006) 164-169.

[12] R.A. Synowicki, B.D. Johs, A.C. Martin, Optical properties of soda-lime float glass from spectroscopic ellipsometry, Thin Solid Films, 519 (2011) 2907-2913.

[13] M. M. Junda, N. J. Podraza, Optical properties of soda lime float glass from 3 mm to 148 nm (0.41 meV to 8.38 eV) by spectroscopic ellipsometry, Surface Science Spectra, 25 (2018) 016001.

[14] M.J. Persky, M. Szczesniak, Infrared, spectral, directional-hemispherical reflectance of fused silica, Teflon polytetrafluoroethylene polymer, chrome oxide ceramic particle surface, Pyromark 2500 paint, Krylon 1602 paint, and Duraflect coating, Applied optics, 47 (2008) 1389-1396.

[15] B.D. Johs, J.A. Woollam, C.M. Herzinger, J.N. Hilfiker, R.A. Synowicki, C.L. Bungay, Overview of variable-angle spectroscopic ellipsometry (VASE): II. Advanced applications, in: Optical Metrology, 1999, pp. 29-58.

[16] D.W. Thompson, B.D. Johs, Infrared ellipsometer/polarimeter system, method of calibration, and use thereof, in, Google Patents, 1998.

[17] K. Gelin, A. Roos, F. Geotti-Bianchini, P. van Nijnatten, Thermal emissivity of coated glazing—simulation versus measurements, Optical Materials, 27 (2005) 705-712.

[18] A.R. Ellis, H.M. Graham, M.B. Sinclair, J.C. Verley, Variable-angle directional emissometer for moderate-temperature emissivity measurements, in: Optical Engineering + Applications, SPIE, 2008, pp. 9.

[19] J. Lohrengel, M. Rasper, F. Geotti-Bianchini, L. De Riu, Angular emissivity at room temperature and spectral reflectance at near normal incidence of float glass, borosilicate glass and glass-ceramics, Glass science and technology, 69 (1996) 64-74.

[20] A. Pantinakis, B. Jones, The accurate measurement of the directional total emittance of uncoated and coated float glass at 283 K, Europhysics Letters, 16 (1991) 545.

[21] J.C. Jonsson, C. Curcija, Inter-laboratory comparison using integrating sphere spectrophotometers to measure reflectance and transmittance of specular, diffuse, and light-redirecting glazing products, in: SPIE Optical Engineering + Applications, SPIE, 2012, pp. 15.